Carbohydrate Polymers 102 (2014) 877–883

Contents lists available at ScienceDirect

Carbohydrate Polymers

journal homepage: www.elsevier.com/locate/carbpol

Facile preparation of magnetic 2-hydroxypropyltrimethyl ammonium chloride chitosan/Fe_3O_4/halloysite nanotubes microspheres for the controlled release of ofloxacin

Qin Wang, Junping Zhang*, Bin Mu, Ling Fan, Aiqin Wang

Center of Eco-material and Green Chemistry, Lanzhou Institute of Chemical Physics, Chinese Academy of Sciences, Lanzhou 730000, PR China

ARTICLE INFO

Article history:
Received 15 August 2013
Received in revised form
29 September 2013
Accepted 21 October 2013
Available online 7 November 2013

Keywords:
Quaternized chitosan
Halloysite
Spray drying
Magnetic microspheres
Controlled release

ABSTRACT

Magnetic microspheres, 2-hydroxypropyltrimethyl ammonium chloride chitosan/Fe_3O_4/halloysite nanotubes/ofloxacin (HACC/Fe_3O_4/HNTs/OFL), for the controlled release of OFL were prepared by *in situ* crosslinking with glutaraldehyde in the spray-drying process. The magnetic microspheres were characterized by Fourier transform infrared spectroscopy, scanning electron microscopy, thermogravimetric analysis and a magnetometer. Various parameters influencing the encapsulation efficiency, drug loading and *in vitro* controlled release properties of the magnetic microspheres for OFL were also studied. Many stripes were formed and some tubular HNTs could be seen at higher magnification on the surface of the HACC/Fe_3O_4/HNTs/OFL magnetic microspheres. The magnetic microspheres show superparamagnetic property and fast magnetic response. The encapsulation efficiency and the cumulative release of OFL are closely related to HACC concentration, HNTs contents and crosslinking density. The release of OFL follows the first-order kinetics.

1. Introduction

2-Hydroxypropyltrimethyl ammonium chloride chitosan (HACC), a quaternized chitosan, is one of water-soluble chitosan derivatives (Cho, Grant, Piquette-Miller, & Allen, 2006). HACC has potential applications in many fields, *e.g.*, drug delivery (Xu, Du, Huang, & Gao, 2003; Xu et al., 2013), orthopedics (Xu, Wang, Guo, Lei, & Tang, 2011), preventing fungal infection of skin (Peng et al., 2010; Sajomsang, Gonil, Saesoo, & Ovatlarnporn, 2012) and nanofiltration (Huang, Chen, Sun, & Gao, 2008; Wang, He, & Che, 2011) due to its biocompatibility, low cytotoxcity, water-solubility, permanent cationic charges, *etc.* In addition, the orally administered HACC could depress the levels of Fe, Zn and Ca in the livers of mice (Wang, Qin, Wang, & Li, 2011). HACC is superior to chitosan in many aspects. For example, the quaternized cationic nature of HACC provides stronger electrostatic interaction with negatively charged tumor cells when it was used as a drug carrier for tumor therapy (Xu et al., 2013). Liu, Luo, et al. (2011) and Liu, Yang, et al. (2011) reported that the lipid-lowering effect of HACC was better than that of carboxymethylated chitosan and chitosan. However, to the best of our knowledge, little information can be seen concerning the preparation of HACC/clay nanocomposites and their applications in drug delivery although HACC is a well-known promising vehicle for drug delivery and superior to chitosan in many aspects.

In recent years, many studied showed that introducing clay minerals into polymer can improve physicochemical properties (such as mechanical properties, thermal stability and bactericidal activity) of the polymeric materials. Also, the introduced clay minerals provide a slower and continuous release of drugs in comparison with pure polymers (Ruiz-Hitzkya et al., 2013; Viseras, Aguzzi, Cerezo, & Bedmar, 2008). Clay minerals including montmorillonite (Liu, Huang, Chang, & Yeh, 2010; Zhao et al., 2010), attapulgite (Wang, Zhang, & Wang, 2009), hydrotalcite (Álvarez, Collazo, Hernández, Nóvoa, & Pérez, 2010), vermiculite (Wang, Xie, Zhang, Zhang, & Wang, 2010) and halloysite nanotubes (HNTs) (Liu, Wu, Jiao, Xiong, & Zhou, 2013) have been used for preparing matrices for controlled drug delivery.

HNTs, a kind of aluminosilicate clay minerals, are chemically similar to kaolin, but morphologically have a hollow tubular structure and the unit layers are separated by a monolayer of water molecules. HNTs are promising natural materials for various biomedical applications such as controlled drug delivery, stem cell attachment and proliferation, and nanoreactors for enzymes immobilization owing to their very low cytotoxicity, good biocompatibility and tubular structure (Veerabadran, Mongayt, Torchilin, Price, & Lvov, 2009; Vergaro et al., 2010). HNTs have also been incorporated in polymers to improve their mechanical properties and

* Corresponding author. Tel.: +86 931 4968251.
E-mail address: jpzhang@licp.cas.cn (J. Zhang).

0144-8617/$ – see front matter © 2013 Elsevier Ltd. All rights reserved.
http://dx.doi.org/10.1016/j.carbpol.2013.10.071

flame retardancy or used to coat corrosion inhibitors for active corrosion protection layers (Rawtani & Agrawal, 2012). For instance, very recent studies demonstrated that the combination of HNTs and chitosan could significantly enhance the tensile properties, storage modulus and glass transition temperature of chitosan (De Silva, Pasbakhsh, Goh, Chai, & Ismail, 2013; Liu, Zhang, Wu, Xiong, & Zhou, 2012). Du, Guo, and Jia (2006) proved that HNTs were a new kind inexpensive, easily processed and effective additive for improving the thermal stability and flame retardant of polypropylene. The introduction of HNTs can significantly reduce the burst release of the drug and improve the tensile strength of the polymer nanofibrous mats compared with pure poly(lactic-*co*-glycolic acid) (Qi et al., 2010).

Here, the magnetic HACC/Fe_3O_4/HNTs/ofloxacin (HACC/Fe_3O_4/HNTs/OFL) microspheres were prepared by spray-drying for the controlled release of OFL as a model drug. OFL is one of a new generation of fluorinated quinolones that is structurally similar to nalidixic acid. It is an orally administered generic antibacterial drug active against most Gram-negative bacteria, many Gram-positive bacteria and some anaerobes (Cui, Zhang, & Tang, 2008). OFL is a zwitterionic compound, and soluble in dilute acetic acid solution and alkali solution, and slightly soluble in water. The crosslinking of HACC by glutaraldehyde was *in situ* accomplished in the spray-drying process. The magnetic microspheres were characterized by Fourier transform infrared spectra (FTIR), scanning electron microscopy (SEM), thermogravimetric analysis (TGA) and a magnetometer. In addition, the effects of various parameters on the encapsulation efficiency (*EE*), drug loading and *in vitro* release of OFL were systematically investigated. Many studies reported that HNTs can reduce the burst release of drugs by trapping drug molecules in the lumen. However, the main aim of introducing HNTs into HACC in this work is to regulate the release of OFL and enhance the bioavailability of the loaded OFL, which is helpful for the application of HACC/Fe_3O_4/HNTs/OFL in the gastro-retentive drug delivery system.

2. Materials and methods

2.1. Materials

HACC with a quaternization degree of 0.32 was supplied by Nantong Lushen Bioengineering Co. Ltd. (Jiangsu, China). HNTs were purchased from Sigma–Aldrich. Fe_3O_4 nanoparticles were purchased from Aladdin Industrial Corporation (Shanghai, China). OFL was purchased from Jiuzhou Pharmaceutical Factory (He'nan, China). All the other reagents used were of analytical grade and all solutions were prepared with distilled water.

2.2. Alkali-activation of HNTs

The alkali-activated HNTs were prepared according to the following procedure. 40.0 g of HNTs powder was suspended in 400 mL of 2 mol/L NaOH solution. The mixture was ultrasonicated at 50 °C for 1 h, and then washed with distilled water until neutrality. The resulting sample was dried at 105 °C to a constant weight and ground into a size of 200-mesh (Wang, Zhang, & Wang, 2013; White, Bavykin, & Walsh, 2012).

2.3. Preparation of magnetic HACC/Fe_3O_4/HNTs/OFL microspheres

The HACC/Fe_3O_4/HNTs/OFL magnetic microspheres were prepared by spray drying. Firstly, a predetermined amount of HACC was dissolved in 350 mL of pH 3.0 acetic acid solution under continuous stirring at 500 rpm, and then an appropriate amount of the Fe_3O_4 nanoparticles were suspended in the solution (suspension I). 0.2 g of OFL was dissolved in 50 mL of pH 3.00 acetic acid solution, and then the alkali-activated HNTs was added with continuous stirring for 12 h to reach the adsorption equilibrium (suspension II). Subsequently, the above-mentioned suspensions (I and II) were mixed under vigorous stirring and the pH was adjusted to 5.0 using 0.1 mol/L NaOH solution. The mixture was stirred at 500 rpm for 12 h at room temperature. Finally, an appropriate amount of glutaraldehyde (0, 1, 2 and 4 mL) was added into the above suspension. After stirred for 30 min, the suspension was spray-dried (Mini Spray Dryer, Type SY1600, China) through a 0.7 mm nozzle at a feed rate of 12 mL/min. The inlet temperature was 150 °C. The gray magnetic microspheres were dried to a constant weight in an oven at 80 °C.

2.4. Determination of EE and drug loading

The magnetic microspheres (0.05 g) were immersed in 50 mL of simulated gastric Fluid (pH 1.2) for 24 h until swelling equilibrium, and then ultrasonicated at 50 °C for 1 h to fully release of OFL from the microspheres. Subsequently, the released OFL from the microspheres was separated from the mixture by centrifugation at 5000 rpm for 20 min. The concentration of OFL was determined using a UV-vis spectrophotometer (SPECORD 200, ANALYTIK JENA AG) at 293 nm. The drug loading (%) and *EE* (%) were calculated using the following equations, respectively.

$$\text{Drug loading}\,(\%) = \frac{\text{Weight of drug in sample}}{\text{Weight of sample}} \times 100 \quad (1)$$

$$EE\ (\%) = \frac{\text{Weight of drug in sample}}{\text{Theoretical weight of drug in sample}} \times 100 \quad (2)$$

2.5. In vitro drug release

In vitro drug release tests were carried out using the USP 30 No. 2 dissolution test apparatus (ZRS-8G, Tianjin University Wireless factory, China) with six rotating paddles. The dialysis bags (MWCO of 8000–14,000 Da) containing the suspension of microspheres (0.1 g) in 5 mL of dissolution medium were placed in 250 mL of the same release medium at 37 °C and stirred at 50 rpm. The dissolution media (pH 1.2, pH 5.0, pH 6.8 and pH 7.4) were prepared by combining HCl, KH_2PO_4 and NaOH solutions properly according to the Chinese Pharmacopoeia 2005. Aliquots of the solutions were collected at the scheduled intervals and filtered with 0.45-μm-pore nylon filters. After each sample collection, the equal amount of fresh release medium at the same temperature was added back. The filtrate was diluted to 10 mL with the fresh release medium. The concentration of OFL was determined by a UV–vis spectrophotometer at the wavelength 293 nm, and then the cumulative release percentage of OFL was determined using Eq. (3):

$$\text{OFL cumulative release}\,(\%) = \frac{R_t}{L} \times 100 \quad (3)$$

where L and R_t represent the initial amount of OFL loaded and cumulative amount of OFL released at time t, respectively.

2.6. Characterization

FTIR spectra of the samples were recorded on a Thermo Nicolet NEXUS TM spectrophotometer using a KBr pellet. Morphology of the samples was observed using scanning electron microscopy (SEM, JSM-5600LV, JEOL Ltd.). The samples for SEM observation were prepared according to the following procedure. The sample was dispersed in ethanol and a drop of the dispersion was put on a copper stub and dried in the open atmosphere. Subsequently, the sample was coated with a thin layer of gold film. The zeta potential was measured using Zetasizer Nano ZS (Malvern Instruments

Table 1
Zeta potentials of HACC, HNTs, OFL and Fe_3O_4 in pH 5.0 aqueous solution.

Samples	HACC	HNTs	OFL	Fe_3O_4
Zeta potentials	39.2 ± 1.77	−31.4 ± 1.52	22.5 ± 1.20	11.1 ± 2.01

Ltd., Worcestershire, UK) by dispersing 0.1 g of the sample in 10 mL pH 5.0 aqueous solution. A vibrating-sample magnetometer (VSM) (Lake Shore, 735 VSM, Model 7304, USA) was used at room temperature to characterize the magnetic properties of the samples. TGA was carried out using a STA 6000 (PerkinElmer Instrument Co. Ltd., USA) to investigate the thermal stability of the samples over a temperature range of 25–800 °C at a rate of 10 °C/min under nitrogen atmosphere.

2.7. Statistical analysis

Statistical analysis for the determination of differences in the adsorption and release characteristics within groups was accomplished using one-way analysis of variance, performed with a statistical program (Origin 8.0). The data were considered to be significantly different at $p < 0.05$. All data are presented as mean values with standard error (mean ± SD). $n = 3$ in each group.

3. Results and discussion

3.1. Preparation of magnetic HACC/Fe_3O_4/HNTs/OFL microspheres

The zeta potentials of HACC, HNTs, Fe_3O_4 and OFL in pH 5.0 solution were determined according to the preparation conditions and are shown in Table 1. The zeta potentials of HACC, Fe_3O_4 and OFL in pH 5.0 solution are 39.2, 11.1 and 22.5 mV, respectively, whereas the zeta potential of HNTs is −31.4 mV. So, there is a strong electrostatic interaction of HNTs with HACC, Fe_3O_4 and OFL in pH 5.0 aqueous suspension. The HACC/Fe_3O_4/HNTs/OFL magnetic microspheres crosslinked by glutaraldehyde were insoluble in water. This is because the amino groups of HACC could couple with —CHO groups of glutaraldehyde in the spray-drying process to form *in situ* crosslinked microspheres. Many studies have also shown that the —CHO groups of glutaraldehyde could couple with the amino groups of HACC to form polymeric networks (Liu & Song, 2012; Wang, He, et al., 2011; Wang, Qin, et al., 2011).

The magnetic property of the HACC/Fe_3O_4/HNTs/OFL magnetic microspheres is shown in Fig. 1. The saturation magnetization of the pure Fe_3O_4 nanoparticles is 52.42 emu/g at 300 K. The saturation magnetization decreases to 33.39 emu/g for the magnetic microspheres because of a large fraction of HACC, HNTs and OFL in the microspheres. The magnetic microspheres can still be operated easily and firmly using a magnet (inset in Fig. 1) indicating favorable magnetic responsivity. Moreover, the hysteresis loop of the magnetic microspheres shows zero coercivity and zero remanence. The results imply that the HACC/Fe_3O_4/HNTs/OFL magnetic microspheres have a superparamagnetic property.

3.2. FTIR analysis

The FTIR spectra of OFL, HNTs, HACC, HACC/Fe_3O_4/OFL, crosslinked HACC/Fe_3O_4/HNTs/OFL and uncrosslinked HACC/Fe_3O_4/HNTs/OFL microspheres are shown in Fig. 2. In Fig. 2c, the absorption peak at 1556 cm^{-1} is attributed to N—H bending of the primary amine (Li, Xiao, & Qin, 2010), suggesting that there is a part of unsubstituted —NH_2 groups in HACC. The absorption peak at 1032 cm^{-1} is due to the C—O stretching vibration (C_3—OH) of HACC (Xu et al., 2013). After crosslinked

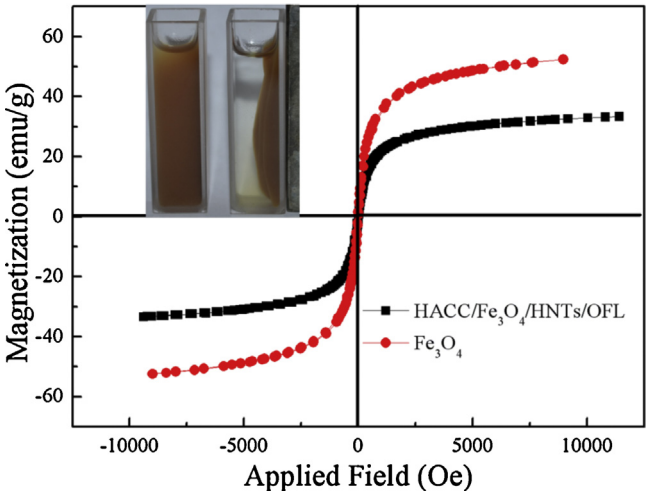

Fig. 1. Magnetic curves of the HACC/Fe_3O_4/HNTs/OFL microspheres (■) and Fe_3O_4 nanoparticles (●).

by glutaraldehyde, the N—H bending of the primary amine at 1556 cm^{-1} becomes weak and slightly shifts to 1552 cm^{-1}, whereas no obvious change was observed for that at 1480 cm^{-1} (Fig. 2d), which further indicates that the crosslinking reaction mainly took place at the C_2—NH sites of the glucosamine units of HACC and the trimethylammonium groups were kept very well during the spay-drying process. Moreover, a new absorption band at 1628 cm^{-1} is detected in the spectrum of HACC/Fe_3O_4/OFL owing to the imine bond (C=N) formed between the amino groups of HACC and the aldehyde groups of glutaraldehyde.

The absorption bands of HNTs at 3693 and 3620 cm^{-1} in Fig. 2b are ascribed to the O—H stretching of HNTs, and the band at 536 cm^{-1} is due to the Si—O bending vibration (Frost, Kristof, Horvath, & Kloprogge, 2000). After incorporated into the magnetic microspheres, these absorption bands slightly shift to 3696, 3618 and 541 cm^{-1} (Fig. 2e) compared with that of HNTs. In addition, the bands of HNTs at 1638 and 911 cm^{-1} are owing to the bending vibration of the adsorbed water and the bending vibration of the inner OH, respectively. These peaks in Fig. 2e could overlap the absorption peaks of HACC at 1644 and 914 cm^{-1}.

In FTIR spectrum of OFL (Fig. 2a), the peaks at 1718 and 1621 cm^{-1} are assigned to the C=O group stretching and N—H bending vibration, respectively. The strong band at 1284 cm^{-1} is ascribed to the stretching vibration of the C—O—C group. The position of these peaks is in accordance with the previous report (Sahoo, Chakraborti, & Behera, 2012). The peak at 1718 cm^{-1} in Fig. 2d is observed when OFL is introduced into magnetic microspheres, but its intensity becomes weaker. In addition, the new peaks at 1584 (carbonyl group of OFL) and 1270 cm^{-1} (C—O—C group of OFL) in the FTIR spectrum of the HACC/Fe_3O_4/OFL magnetic microspheres (Fig. 2d) are also found in Fig. 2e–g. These results indicate that OFL was successfully entrapment in the magnetic microspheres. Compared with the FTIR spectrum in Fig. 2f, the intensity of the peak at 1714 cm^{-1} in Fig. 2g is stronger, indicating that the there is a interaction between C=O groups of OFL and glutaraldehyde.

3.3. Morphology

The surface morphology of HACC/Fe_3O_4/OFL, HACC/Fe_3O_4/10% HNTs/OFL and HACC/Fe_3O_4/40% HNTs/OFL magnetic microspheres was observed by SEM (Fig. 3). The surface of the HACC/Fe_3O_4/OFL magnetic microsphere is smooth (Fig. 3a and a′). The surface becomes rough when HNTs were introduced (Fig. 3b, b′, c and c'). In addition, many stripes were formed on the surface of the

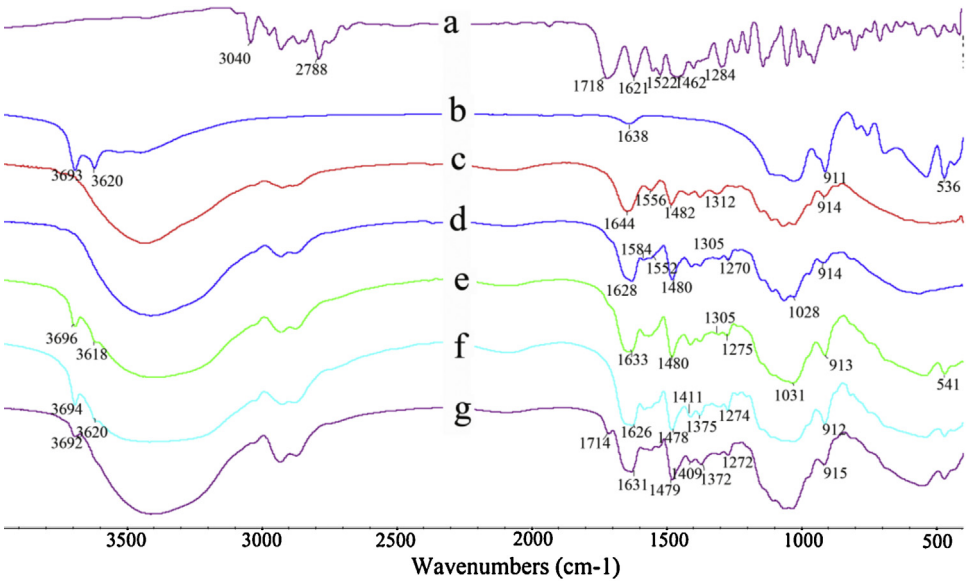

Fig. 2. FTIR spectra of (a) OFL, (b) HNTs (c) HACC, (d) HACC/Fe_3O_4/OFL, (e) HACC/Fe_3O_4/10%HNTs/OFL, (f) HACC/Fe_3O_4/40%HNTs/OFL and (g) uncrosslinked HACC/Fe_3O_4/40%HNTs/OFL.

HACC/Fe_3O_4/HNTs/OFL magnetic microspheres in comparison with the HACC/Fe_3O_4/OFL microspheres. Some tubular HNTs can be seen at higher magnification (Fig. 3b′ and c′) on the surface of the microspheres. However, the sphericity of the microspheres with higher HNTs content is worse than that of the HACC/Fe_3O_4/OFL magnetic microspheres. The changes in surface morphology may have some influences on the release of OFL from the microspheres.

3.4. Thermal stability

TGA curves of the magnetic microspheres are shown in Fig. 4. As can be seen, the weight loss of the HACC/Fe_3O_4/OFL magnetic microspheres is lower than that of the HACC/Fe_3O_4/HNTs/OFL magnetic microspheres at temperature below 100 °C. This is because of the physisorbed water of the introduced HNTs. The weight loss of the magnetic microspheres between 250 and 430 °C increases with incorporating 5% HNTs, but decreases with further increasing the HNTs content from 10 to 40%. This means the incorporation of a higher content of HNTs is helpful to improve thermal stability of the magnetic microspheres because the HNTs act as heat barriers and decrease the diffusion of volatile products (Zheng & Wang, 2010).

The differential scanning calorimetry (DSC) curves is also shown in Fig. 4 (inset). There is one exothermal peak in the decomposition process in the temperature range of 200 to 500 °C. The DSC curves are consistent with the TGA curves. This is attributed to decomposition of HACC.

3.5. Adsorption and release for OFL

The *EE* and drug loading of the magnetic microspheres with different HACC concentration are shown in Table 2. The drug loading decreases, whereas there is no significant difference in the *EE* with

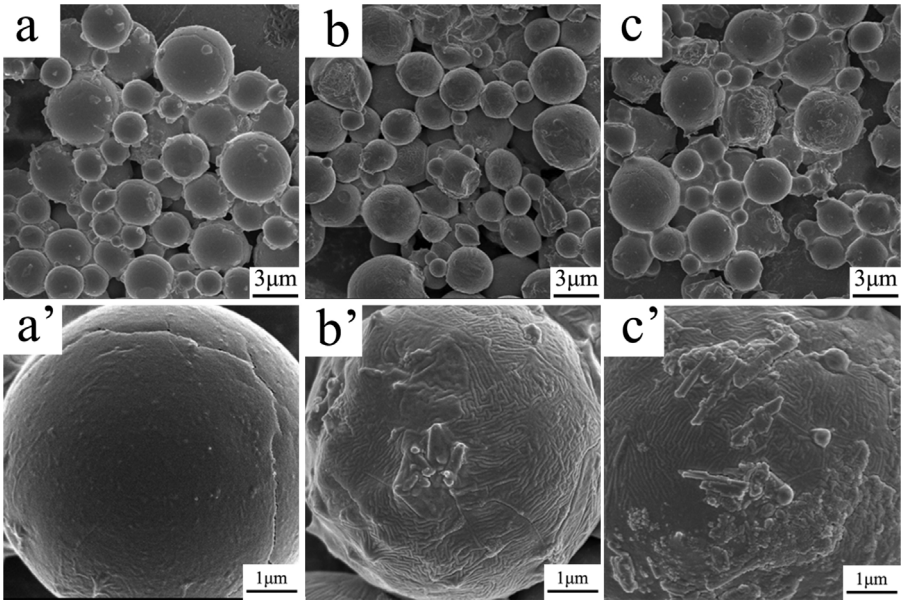

Fig. 3. SEM images of (a and a′) HACC/Fe_3O_4/OFL, (b and b′) HACC/Fe_3O_4/10%HNTs/OFL and (c and c′) HACC/Fe_3O_4/40%HNTs/OFL magnetic microspheres.

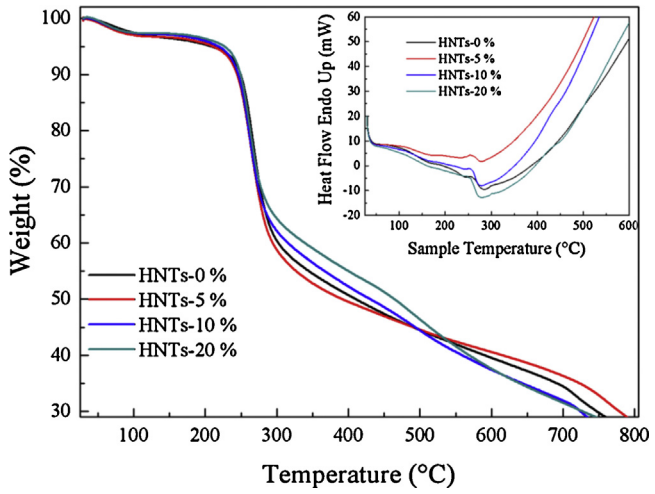

Fig. 4. TGA and DSC curves of the magnetic microspheres with different HNTs content.

Table 2
Variation of drug loading and *EE* of the magnetic microspheres with HACC concentration, HNTs content and glutaraldehyde concentration.

Parameters		Drug loading (%)	*EE* (%)
HACC conc. (%)	0.5	6.04 ± 0.17	88.49 ± 2.17
	1.0	3.54 ± 0.15	87.57 ± 2.57
	1.5	2.65 ± 0.01	91.98 ± 1.10
	2.0	1.95 ± 0.05	87.48 ± 1.13
HNTs content (%)	0	7.27 ± 0.10	91.89 ± 0.65
	5	6.79 ± 0.18	90.16 ± 1.21
	10	6.29 ± 0.16	87.29 ± 1.09
	20	5.69 ± 0.05	85.81 ± 0.34
	40	5.08 ± 0.04	84.42 ± 0.39
Glutaraldehyde conc. (%)	0	6.55 ± 0.13	95.68 ± 0.96
	0.25	6.30 ± 0.13	87.53 ± 0.93
	0.50	6.09 ± 0.06	89.27 ± 0.41
	1.00	5.86 ± 0.01	86.39 ± 0.03

increasing the HACC concentration ($p > 0.05$). In addition, the cumulative release of OFL in pH 1.2 solution decreases with increasing the HACC concentration (Fig. 5a). The result from Fig. 2 shows that the amino groups of HACC could react with —CHO groups of glutaraldehyde *via* the Schiff base reaction to form a polymeric network. The crosslinking density of the microspheres increases with increasing HACC concentration, which could restrict the emigration of OFL from the magnetic microspheres, and then decrease the release rate of OFL.

As can also be seen from Table 2, the drug loading and the *EE* decrease with increasing the HNTs content, and there are significant differences of the drug loading and the *EE* with increasing the HNTs content ($p < 0.05$). The tendency may be attributed to the following facts. HACC can sufficiently react with glutaraldehyde to form a compact network when the HNTs content is 0%, which is of benefit for the encapsulation of OFL in the magnetic microspheres. When HNTs are introduced into the HACC solution, the well-dispersed tubular HNTs may hinder the Schiff base reaction

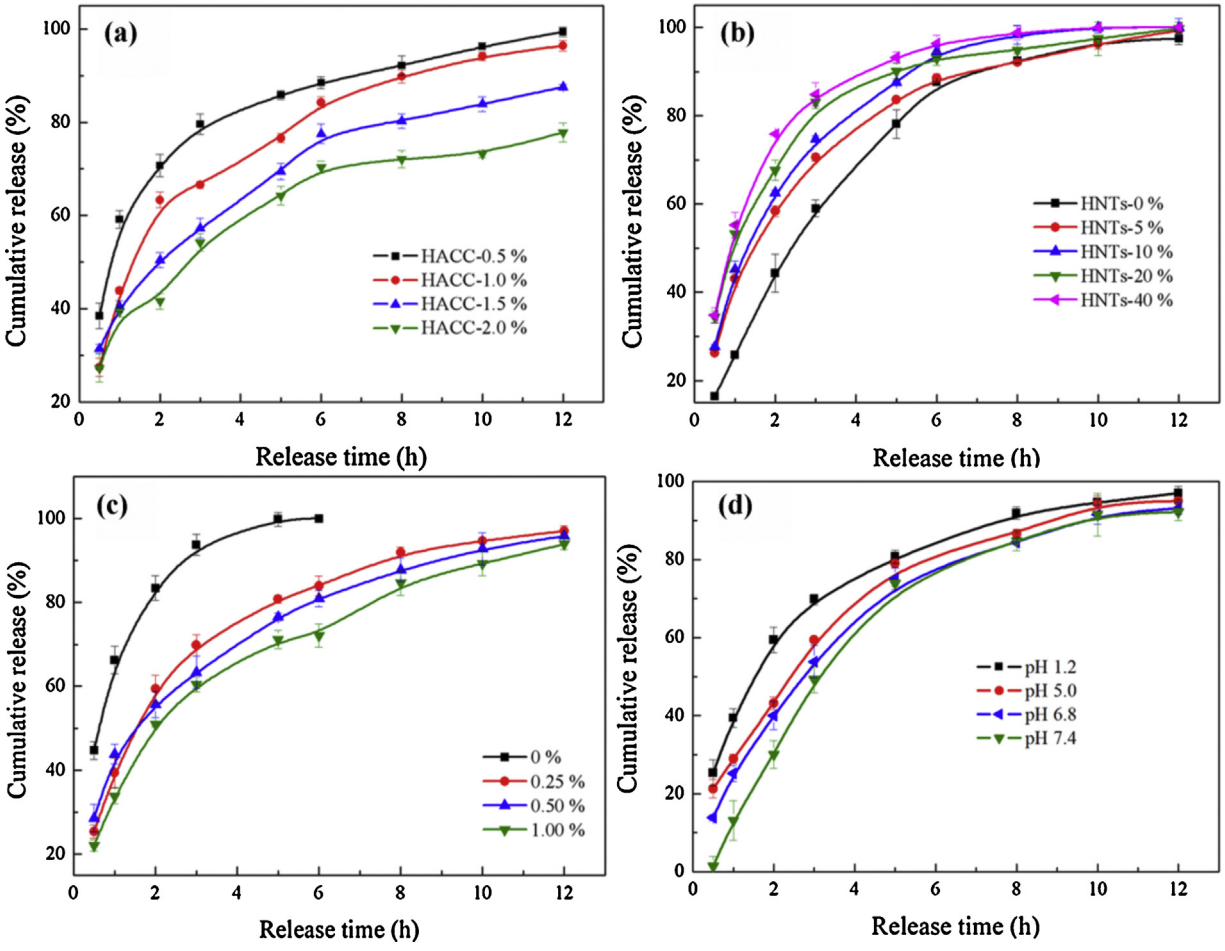

Fig. 5. Variations of cumulative release of OFL from the magnetic microspheres with (a) HACC concentration, (b) HNTs content, (c) glutaraldehyde concentration, (d) pH in the release medium.

between HACC and glutaraldehyde. Consequently, a loose network was formed, which results in the decrease of the *EE* though an increase in HNTs content is conducive to the adsorption of HNTs for OFL.

Fig. 5b presents the effect of HNTs content on the cumulative release of OFL in pH 1.2 solution. The HNTs content can regulate OFL release from the HACC/Fe_3O_4/OFL magnetic microspheres at pH 1.2. The OFL cumulative release ratio is 78.14% after 5 h which is the gastric emptying time. The OFL cumulative release ratio increases to 84% after 5 h when 5% HNTs are introduced. With increasing HNTs content, the OFL cumulative release ratio further increases. This result indicates that introducing HNTs can accelerate the release of OFL in the stomach and increase the bioavailability of loaded OFL. This tendency is consistent with that of the *EE*. The crosslinking density decreases with increasing the HNTs content from 0 to 40% because HNTs could hinder the reaction between HACC and glutaraldehyde. In addition, the rougher surface at higher HNTs content (Fig. 3) is also of benefit for the release of OFL from the HACC/Fe_3O_4/HNTs/OFL magnetic microspheres. Thus, an increase in the cumulative release of OFL with increasing the HNTs content was observed.

The *EE* and drug loading of the magnetic microspheres with different glutaraldehyde concentration are also shown in Table 2. The drug loading decreases with increasing the glutaraldehyde concentration. The *EE* decreases when 0.25% glutaraldehyde was introduced. However, no significant difference in *EE* was detected with increasing the glutaraldehyde concentration from 0.25 to 1.00% ($p > 0.05$). The cumulative release of OFL evidently decreases when 0.25% glutaraldehyde was introduced, and then decreases with further increasing the glutaraldehyde concentration to 1.00% (Fig. 5c). Without glutaraldehyde, the microspheres are only formed *via* electrostatic interaction and hydrogen bonding. Thus, very fast release of OFL was observed. The microspheres were chemically crosslinked when glutaraldehyde was introduced and the crosslinking density increases with increasing the glutaraldehyde concentration. Consequently, the diffusion of the loaded OFL into the dissolution media was slowed down (Kulkarni, Kulkarni, & Keshavayya, 2007; Mi, Kuan, Shyu, Lee, & Chang, 2000).

pH is a key factor influencing the oral drug delivery. It is known that pH is about 1.2 ~ 2.0 in stomach, about 7.0 in small intestine and as high as 8.0 in the distal part (Shargel & Yu, 1999). The effect of pH on the release rate of OFL from the magnetic microspheres is shown in Fig. 5d. As can be seen, the cumulative release of OFL from the magnetic microspheres is above 90% at the end of the experiment (12 h) regardless of the pH of solutions. However, there are significant differences in cumulative release in different pH solution ($p < 0.05$). The significant difference in cumulative release in different pH solutions is attributed to the following facts. The difference in solubility of OFL at different pH is one of the reasons for the difference in drug release. OFL molecules (pKa_1 6.08 and pKa_2 8.25) exist as cationic, neutral and anionic species in acidic, neutral and alkaline solutions, respectively (Goyne, Chorover, Kubicki, Zimmerman, & Brantley, 2005). OFL molecules exist as cationic species when pH < 3.16, cationic and neutral species when pH 3.16–6.96, neutral species when pH 6.96–7.22, neutral and anionic species when pH 7.22–9.12, and anionic species when pH > 9.12 (Huang, Deng, & Xu, 2010). Therefore, it is easy for the OFL to migrate out of the magnetic microspheres at pH 1.2 because OFL is soluble in acidic solution, which leads to a higher cumulative release compared with that at pH 5.0, 6.8 and 7.4. Compared with pH 6.8, more of the OFL molecules are in the cationic form at pH 5.0. So, the cumulative release at pH 5.0 is higher than that at pH 6.8. Because there is a part of cationic species at pH 6.8 solution and a part of anionic species at pH 7.4 solution, the cumulative release of OFL at pH 6.8 and 7.4 solutions reaches 90% or so at the end of the experiment (12 h). However, no significant difference of the cumulative release rates at both pH 6.8 and 7.4 was detected ($p > 0.05$). The interaction of OFL and the microspheres is another reason for the difference in drug release behavior. The isoelectric point of HNTs is around pH 3.0 (Guimaraês, Enyashin, Seifert, & Duarte, 2010), indicating that HNTs are positively charged at pH < 3.0. The zeta potential of OFL in acid solution is positive due to the protonation of amino groups of OFL. Therefore, the electrostatic repulsion between halloysite and OFL at pH = 1.2 can also accelerate the release of OFL from the magnetic microspheres. Considering the gastric emptying time (5–6 h) and the drug cumulative release ratio at pH 1.2 after 6 h, the HACC/Fe_3O_4/HNTs/OFL magnetic microspheres are suitable for the gastro-retentive drug delivery system.

Table 3
Kinetic parameters for the release of OFL from the magnetic microspheres in different pH solutions.

pH	Zero-order		First-order		Higuchi		Power law		
	k_1	r_1^2	k_2	r_2^2	k_3	r_3^2	n	k_4	r_4^2
1.2	5.56	0.82	0.27	0.99	25.19	0.93	0.41	39.08	0.95
5.0	6.38	0.88	0.25	0.98	28.42	0.96	0.50	30.83	0.98
6.8	6.75	0.88	0.23	0.99	30.04	0.97	0.60	24.49	0.97
7.4	7.64	0.88	0.22	0.99	34.03	0.96	1.17	8.09	0.86

In order to further study the release behavior of OFL from the magnetic microspheres in different pH solution, the *in vitro* release data in different pH solutions were fitted to various models to analyze the kinetics and the release mechanism of OFL. The experimental data was analyzed using zero-order equation (4), first-order equation (5) (Gibaldi & Feldman, 1967; Wagner, 1969), Higuchi's square root model (6) (Higuchi, 1963), and the Power law (7) (Ritger & Peppas, 1987; Siepmann & Peppas, 2001) to elucidate the release kinetics of OFL. Where, F_t is the drug release fraction at time "t", k_1–k_4 are the release constants of the respective equations, t is the release time, and n is the characteristic diffusion exponent.

$$F_t = k_1 t \quad (4)$$

$$F_t = 1 - e^{-k_2 t} \quad (5)$$

$$F_t = k_3 t^{1/2} \quad (6)$$

$$F_t = k_4 t^n \quad (7)$$

The correlation coefficient (r_2^2) for Eq. (5) is above 0.98 at different pH solutions (Table 3). This is obviously higher than the other kinetic equations, *e.g.*, zero-order, Higuchi equation and the Power law, suggesting that the release mode of OFL follows the first-order kinetics.

4. Conclusions

The magnetic HACC/Fe_3O_4/HNTs/OFL microspheres with controlled release properties were prepared by a facile spray-drying technique. The magnetic microspheres possess superparamagnetic property and fast magnetic response. The results from FTIR spectra indicate that the amino groups of HACC could react with —CHO groups of glutaraldehyde *via* the Schiff base reaction to form polymeric network. HNTs have remarkable effect on the roughness of the surface, which decreases the *EE* and accelerates the release of OFL though an increase in HNTs content is conducive to the adsorption of HNTs for OFL. However, the introduction of HNTs can improve the bioavailability of OFL in the gastro-retentive drug delivery system. The crosslinking density of the polymeric network has an effect on the *EE* and cumulative release. The effect of pH of the release media on the release rate of OFL is related to the state of OFL molecules and the interaction between OFL and the microspheres. The release of OFL in different pH solution follows the first-order

kinetics. The magnetic microspheres are promising to be used as carriers for magnetically driven targeted delivery of drugs in the upper intestinal tract.

Acknowledgements

We are grateful for financial support of the National Natural Science Foundation of China (No. 51003112) and the "Hundred Talents Program" of the Chinese Academy of Sciences.

References

Álvarez, D., Collazo, A., Hernández, M., Nóvoa, X. R., & Pérez, C. (2010). Characterization of hybrid sol–gel coatings doped with hydrotalcite-like compounds to improve corrosion resistance of AA2024-T3 alloys. *Progress in Organic Coatings*, *68*, 91–99.

Cui, Y., Zhang, Y., & Tang, X. (2008). In vitro and *in vivo* evaluation of OFL sustained release pellets. *International Journal of Pharmaceutics*, *360*, 47–52.

Cho, J., Grant, J., Piquette-Miller, M., & Allen, C. (2006). Synthesis and physicochemical and dynamic mechanical properties of a water-soluble chitosan derivative as a biomaterial. *Biomacromolecules*, *7*, 2845–2855.

De Silva, R. T., Pasbakhsh, P., Goh, K. L., Chai, S. P., & Ismail, H. (2013). Physico-chemical characterisation of chitosan/halloysite composite membranes. *Polymer Test*, *32*, 265–271.

Du, M. L., Guo, B. C., & Jia, D. M. (2006). Thermal stability and flame retardant effects of halloysite nanotubes on poly(propylene). *European Polymer Journal*, *42*, 1362–1369.

Frost, R. L., Kristof, J., Horvath, E., & Kloprogge, J. T. (2000). Rehydration and phase changes of potassium acetate-intercalated halloysite at 298 K. *Journal of Colloid and Interface Science*, *226*, 318–327.

Guimaraês, L., Enyashin, A. N., Seifert, G., & Duarte, H. A. (2010). Structural, electronic, and mechanical properties of single-walled halloysite nanotube models. *Journal of Physical Chemistry C*, *114*, 11358–11363.

Gibaldi, M., & Feldman, S. (1967). Establishment of sink conditions in dissolution rate determinations-theoretical considerations and application to nondisintegrating dosage forms. *Journal of Pharmaceutical Sciences*, *56*, 1238–1242.

Goyne, K. W., Chorover, J., Kubicki, J. D., Zimmerman, A. R., & Brantley, S. L. (2005). Sorption of the antibiotic ofloxacin to mesoporous and nonporous alumina and silica. *Journal of Colloid and Interface Science*, *283*, 160–170.

Higuchi, T. (1963). Mechanism of sustained-action medication. Theoretical analysis of rate of release of solid drugs dispersed in solid matrices. *Journal of Pharmaceutical Sciences*, *52*, 1145–1149.

Huang, Q. L., Deng, Y. P., & Xu, S. Y. (2010). Determination of dissociation constants of ofloxacin by UV spectrophotometry. *China Pharmacy*, *21*, 3907–3909.

Huang, R. H., Chen, G. H., Sun, M. K., & Gao, C. J. (2008). Preparation and characterization of quaterinized chitosan/poly(acrylonitrile) composite nanofiltration membrane from anhydride mixture cross-linking. *Separation and Purification Technology*, *58*, 393–399.

Kulkarni, V. H., Kulkarni, P. V., & Keshavayya, J. (2007). Glutaraldehyde-crosslinked chitosan beads for controlled release of diclofenac sodium. *Journal of Applied Polymer Science*, *103*, 211–217.

Li, W., Xiao, L., & Qin, C. Q. (2010). Synthesis and relevant electrochemical properties of 2-hydroxypropyl trimethyl ammonium chloride chitosan-grafted multi-walled carbon nanotubes. *Journal of Materials Science*, *45*, 5915–5922.

Liu, C., Luo, Y. F., Jia, Z. X., Zhong, B. C., Li, S. Q., Guo, B. C., et al. (2011). Enhancement of mechanical properties of poly(vinyl chloride) with polymethyl methacrylate-grafted halloysite nanotube. *eXPRESS Polymer Letters*, *5*, 591–603.

Liu, G. Q., & Song, J. Y. (2012). Electroresponsive behavior of 2-hydroxypropyltrimethyl ammonium chloride chitosan/poly(vinyl alcohol) interpenetrating polymer network hydrogel. *Polymer International*, *61*, 596–601.

Liu, M. X., Zhang, Y., Wu, C. C., Xiong, S., & Zhou, C. R. (2012). Chitosan/halloysite nanotubes bionanocomposites: Structure, mechanical properties and biocompatibility. *International Journal of Biological Macromolecules*, *51*, 566–575.

Liu, M. X., Wu, C. C., Jiao, Y. P., Xiong, S., & Zhou, C. R. (2013). Chitosan–halloysite nanotubes nanocomposite scaffolds for tissue engineering. *Journal of Materials Chemistry B*, *1*, 2078–2089.

Liu, S. P., Huang, I. J., Chang, K. C., & Yeh, J. M. (2010). Mechanical properties of polystyrene-montmorillonite nanocomposites—Prepared by melt intercalation. *Journal of Applied Polymer Science*, *115*, 288–296.

Liu, X. F., Yang, F., Song, T., Zeng, A., Wang, Q., Sun, Z., et al. (2011). Synthesis of carboxymethylated and quaternized chitosans and their therapeutic effect on nonalcoholic fatty liver disease. *Journal of Agricultural and Food Chemistry*, *59*, 10683–10692.

Mi, F. L., Kuan, C. Y., Shyu, S. S., Lee, S. T., & Chang, S. F. (2000). The study of gelation kinetics and chain-relaxation properties of glutaraldehyde-cross-linked chitosan gel and their effects on microspheres preparation and drug release. *Carbohydrate Polymers*, *41*, 389–396.

Peng, Z. X., Wang, L., Dua, L., Guo, S. R., Wang, X. Q., & Tang, T. T. (2010). Adjustment of the antibacterial activity and biocompatibility of hydroxypropyltrimethyl ammonium chloride chitosan by varying the degree of substitution of quaternary ammonium. *Carbohydrate Polymers*, *81*, 275–283.

Qi, R., Guo, R., Shen, M., Cao, X., Zhang, L., Xu, J., et al. (2010). Electrospun poly(lactic-co-glycolic acid)/halloysite nanotube composite nanofibers for drug encapsulation and sustained release. *Journal of Materials Chemistry*, *20*, 10622–10629.

Rawtani, D., & Agrawal, Y. K. (2012). Multifarious applications of halloysite nano tubes: A review. *Reviews on Advanced Materials Science*, *30*, 282–295.

Ritger, P. L., & Peppas, N. A. (1987). A simple equation for description of solute release. I: Fickian and non-Fickian release from non-swellable devices in the form of slabs, spheres, cylinders or discs. *Journal of Controlled Release*, *5*, 23–36.

Ruiz-Hitzkya, E., Dardera, M., Fernandes, F. M., Wicklein, B., Alcântaraa, A. C. S., & Aranda, P. (2013). Fibrous clays based bionanocomposites. *Progress in Polymer Science*, *38*, 1392–1414.

Sahoo, S., Chakraborti, C. K., & Behera, P. K. (2012). FTIR and Raman spectroscopic investigations of ofloxacin/carbopol940 mucoadhesive suspension. *International Journal of PharmTech Research*, *4*, 382–391.

Sajomsang, W., Gonil, P., Saesoo, S., & Ovatlarnporn, C. (2012). Antifungal property of quaternized chitosan and its derivatives. *International Journal of Biological Macromolecules*, *50*, 263–269.

Shargel, L., & Yu, A. (1999). *Applied biopharmaceutics and pharmacokinetics*. New York: McGraw Hill.

Siepmann, J., & Peppas, N. A. (2001). Modeling of drug release from delivery systems based on hydroxypropyl methylcellulose (HPMC). *Advanced Drug Delivery Reviews*, *48*, 139–157.

Veerabadran, N. G., Mongayt, D., Torchilin, V., Price, R. R., & Lvov, Y. M. (2009). Organized shells on clay nanotubes for controlled release of macromolecules. *Macromolecular Rapid Communications*, *30*, 99–103.

Vergaro, V., Abdullayev, E., Lvov, Y. M., Zeitoun, A., Cingolani, R., Rinaldi, R., et al. (2010). Cytocompatibility and uptake of halloysite clay nanotubes. *Biomacromolecules*, *11*, 820–826.

Viseras, C., Aguzzi, C., Cerezo, P., & Bedmar, M. C. (2008). Biopolymer–clay nanocomposites for controlled drug delivery. *Materials Science and Technology*, *24*, 1020–1026.

Wagner, J. G. (1969). Interpretation of percent dissolved-time plots derived from in vitro testing of conventional tablets and capsules. *Journal of Pharmaceutical Sciences*, *58*, 1253–1257.

Wang, J. L., He, R. H., & Che, Q. T. (2011). Anion exchange membranes based on semi-interpenetrating polymer network of quaternized chitosan and polystyrene. *Journal of Colloid and Interface Science*, *361*, 219–225.

Wang, L. S., Qin, C. Q., Wang, W., & Li, W. (2011). Effect of orally administered *N*-(2-hydroxyl) propyl-3-trimethyl ammonium chitosan on the levels of iron, zinc, copper, calcium and lead in mice. *Carbohydrate Polymers*, *84*, 1289–1292.

Wang, Q., Xie, X. L., Zhang, X. W., Zhang, J. P., & Wang, A. Q. (2010). Preparation and swelling properties of pH sensitive composite hydrogel beads based on chitosan-*g*-poly (acrylic acid)/vermiculite and sodium alginate for diclofenac controlled release. *International Journal of Biological Macromolecules*, *46*, 356–362.

Wang, Q., Zhang, J. P., & Wang, A. Q. (2009). Preparation and characterization of a novel pH sensitive chitosan-*g*-poly (acrylic acid)/attapulgite/sodium alginate composite hydrogel bead for controlled release of diclofenac sodium. *Carbohydrate Polymers*, *78*, 731–737.

Wang, Q., Zhang, J. P., & Wang, A. Q. (2013). Alkali activation of halloysite for adsorption and release of ofloxacin. *Applied Surface Science*, *287*, 54–61.

White, R. D., Bavykin, D. V., & Walsh, F. C. (2012). The stability of halloysite nanotubes in acidic and alkaline aqueous suspensions. *Nanotechnology*, *23*, 065705 (10 pp.).

Xu, X. F., Li, Y. G., Wang, F. H., Lv, L., Liu, J. Y., Li, M. N., et al. (2013). Synthesis, in vitro and in vivo evaluation of new norcantharidin-conjugated hydroxypropyltrimethyl ammonium chloride chitosan derivatives as polymer therapeutics. *International Journal of Pharmaceutics*, *453*, 610–619.

Xu, X. F., Wang, L., Guo, S. G., Lei, L., & Tang, T. T. (2011). Surface chemical study on the covalent attachment of hydroxypropyltrimethyl ammonium chloride chitosan to titanium surfaces. *Applied Surface Science*, *257*, 10520–10528.

Xu, Y. M., Du, Y. M., Huang, R. H., & Gao, L. P. (2003). Preparation and modification of *N*-(2-hydroxyl) propyl-3-trimethylammonium chitosan chloride nanoparticle as a protein carrier. *Biomaterials*, *24*, 5015–5022.

Zhao, F., Bao, X. J., McLauchlin, A. R., Gu, J. J., Wan, C. Y., & Kandasubramanian, B. (2010). Effec of POSS on morphology and mechanical properties of polyamide 12/montmorillonite nanocomposites. *Applied Clay Science*, *47*, 249–256.

Zheng, Y. A., & Wang, A. Q. (2010). Enhanced adsorption of ammonium using hydrogel composites based on chitosan and halloysite. *Journal of Macromolecular Science A*, *47*, 33–38.